Relationship between the Charge Distribution and Dipole Moment Functions of CO and the Related Molecules CS, SiO, and SiS

James F. Harrison*

Department of Chemistry, Michigan State University, East Lansing, Michigan 48824-1322

Received: October 26, 2005

The dipole moment functions of the titled molecules are written as the sum of a charge and induced atomic dipole contribution and the distance dependence interpreted in terms of these components. These two contributions have opposite signs over a large range of internuclear distances, and when they have equal magnitudes, the dipole moment vanishes. This happens with CO near the equilibrium bond length and is responsible for its small dipole moment. The dipole moment of CS is $0.770ea_0$, rather large for a diatomic in which the two atoms have essentially the same electronegativities; this is because for CS, the two components of the dipole moment have the same sign at equilibrium and reinforce one another.

Preface

One of the most significant developments in computational chemistry over the past few decades is the ability to construct wave functions for moderately sized systems that allow for the prediction of many molecular properties to chemical accuracy.[1−5] If this symbiosis between method development and computational implementation[6] continues at its present rate, one expects the size of the systems that can be treated accurately will continue to grow and our understanding of molecular properties will be considerably deepened. An interesting question is how the detailed information contained in accurate molecular wave functions will be mapped onto chemical concepts, such as the charge distribution in a molecule, that have and will continue to serve us well. Although the notion that an atom in a molecule carries a net charge is a cornerstone of modern chemistry, efforts to quantify these charges have met with limited success.

Because the in situ charge on an atom is not an observable, any attempt to assign a value to it must involve a model of some sort, and a particularly attractive class of models are those that assume that the molecular electron density, η^{mol}, may be partitioned among the various atoms as in $\eta^{\mathrm{mol}} = \sum_{k=1}^{\mathrm{nuclei}} \eta_k^{\mathrm{atom}}$. Methods such as Mulliken's[7] population analysis and Stone's[8,9] distributed multipole analysis allocate the density to various atoms on the basis of an algorithm that is basis set dependent; the algorithm may predict charges that do not converge in sync with the electron density. Mulliken's method is very sensitive[10−13] to the basis set used; in contrast, Stone's is rather robust, having little or no problems with diatomics[14] but exhibiting an increased sensitivity when applied to polyatomics with basis sets containing the diffuse functions often used in modern computational chemistry. We note that Stone[15] has recently published a modification of his originally distributed multipole moment analysis that is designed to alleviate this basis set dependence.

Other methods focus on the electron density directly and, accordingly, are less sensitive to vagaries of the basis set; these methods fall into two broad classes that may be characterized by having either nonoverlapping or overlapping atomic densities. In the nonoverlapping class, the in situ atomic densities are disjointed in the sense that one assigns regions of space to an individual atom using a Voronoi[16,17] or Bader[18] partitioning, and whatever density is in that region belongs to that atom. This method of defining an in situ atom is compelling because of the exclusivity of the partitioning and the similarity to the ubiquitous space filling representations of molecules. However, the exclusivity of the partitioning is somewhat unphysical in the sense that if one were to take a diatomic molecule and turn off the interactions between the two centers the sum of the resulting noninteracting atomic densities would look very similar to the molecular density. The electron density on one atom would have a significant value at the nucleus of the second atom, suggesting that one should consider a partitioning in which the in situ atoms have overlapping charge densities.

A method of defining a molecular density as a collection of overlapping atomic densities was suggested by Hirshfeld[17,19,20] and is the method we will investigate in this report. Hirshfeld defines a proto-molecule as a collection of noninteracting or free atoms located at the appropriate equilibrium positions in the molecule of interest. The corresponding proto-molecule density is simply the sum of the free atom densities, $\eta^{\mathrm{pm}} = \sum_{k=1}^{\mathrm{nuclei}} \eta_k^0$, where η_k^0 is the free atom density on the center k. He suggested that, if one wants to partition the electron density in a molecule among the various atomic centers, one should allocate the molecular density at a point in the molecule to the constituent atoms in proportion to the fraction of the corresponding free atom density to the proto-molecule density at this point. This fraction is $W_k = (\eta_k^0/\eta^{\mathrm{pm}})$, and an in situ atomic density is given by $\eta_k = W_k\eta^{\mathrm{mol}}$ with the number of electrons associated with the center k given by the integral over η_k. A consequence of representing the molecular density as a sum of in situ atomic densities is that most multiplicative one-electron properties, such as the molecular multipole moments, will be a sum of atomic contributions.[21] We will use these ideas to analyze the bond length dependence of the electron distribution and dipole moment in CO and the related molecules CS, SiO, and SiS.

Introduction

The experimental values for the dipole moments (both magnitude and polarity) of CO,[22] CS,[23] SiO,[24] and SiS,[25] equilibrium bond length,[26] and the electronegativity difference[27] (on three different scales) of the constituent atoms are listed in Table 1. Our sign convention is that the dipole moment of a diatomic AB is considered positive if the polarity is A^- B^+. CO and CS stand out immediately. CO stands out because its

* E-mail: harrison@chemistry.msu.edu. Fax: 517-353-9715. Phone: 517-355-9715 X 295.

10.1021/jp058279z CCC: $33.50
Published on Web 08/30/2006

TABLE 1: Experimental Dipole Moments, Bond Lengths, and Electronegativity Differences

molecule AB	electronegativity difference ($\chi_A - \chi_B$)[a]			μ (ea_0)[b]	R_{eq} (a_0)[c]
	Allen	Pauling	Mulliken		
C^-O^+	1.07	0.89	0.55	+0.043	2.132
C^-S^+	0.05	0.03	−0.02	+0.770	2.909
Si^+O^-	1.69	1.54	1.19	−1.215	2.854
Si^+S^-	0.67	0.68	0.62	−0.681	3.645

[a] Reference 27. [b] Experimental dipole moments: CO,[22] CS,[23] SiO,[24] and SiS.[25] [c] Reference 26.

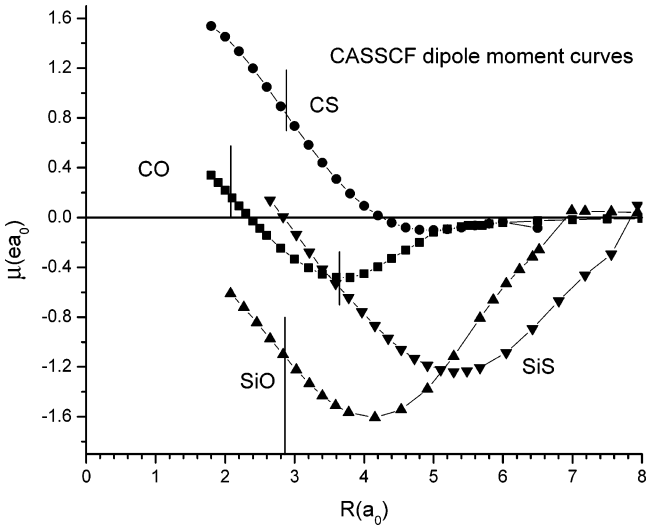

Figure 1. Dipole moment functions for CO, CS, SiO, and SiS calculated with a CASSCF wave function using an aug-cc-pV5Z basis. The vertical lines identify the experimental equilibrium internuclear distance.

dipole moment has the polarity C^-O^+, which is opposite to what one would expect from electronegativity arguments. CS stands out because it has a large dipole moment with the polarity C^-S^+ even though C and S have comparable electronegativities. Additionally, from the dipole moment function shown in Figure 1 , we see that CO, CS, and SiS have a range of bond lengths in which they have a polarity opposite to that expected from electronegativity arguments.[28] CO is the most widely known as it changes sign in the region of its equilibrium bond length; in contrast, CS changes sign at distances larger than the equilibrium bond length. SiS, in contrast, changes sign at bond lengths that are significantly smaller than the equilibrium bond length, and apparently, SiO behaves similarly. We are interested in exploring the reasons for this behavior and in particular the relationship between the charge on the constituent atoms and the dipole moment.

Our approach is to write the dipole moment as[19,20,29] $\mu = -\int z\delta\eta(\vec{r})\ dV$ where the internuclear line defines the z axis and $\delta\eta$ is the density difference function. Then, using the Hirshfeld[19] method, we partition $\delta\eta$ into contributions from the two atoms, permitting us to express the dipole moment of a diatomic AB as $\mu = q(B)R + \mu_A + \mu_B$. q(B) is the charge on atom B, and μ_A and μ_B are the induced dipole moments on atoms A and B. We show (vide infra) that the dipole moment function changes sign because there is an R at which the charge contribution q(B)-R is negative and the sum of the induced atomic dipoles $\mu_A + \mu_B$ is positive, and they cancel. In what follows, we will discuss the electronic structure of these molecules, the equation $\mu = q(B)R + \mu_A + \mu_B$, and then the charge distribution and induced dipoles in the individual molecules. There are several detailed calculations of dipole moments[5,30,31] of the titled molecules, and our emphasis in this work is on the physical content of the dipole moment rather than on its detailed value. There are two previous studies[17,20] of the Hirshfeld charge distribution in the titled molecules at their equilibrium bond length, one using the restricted Hartree−Fock (RHF) wave function[20] and one being a density function theory (DFT) study[17] using the B3LYP functional. The RHF study also reports the induced atomic moments. We will compare these results with ours subsequently.

Electronic Structure. Each of the molecules of interest is formed from two ^3P_g atoms, and we will discuss CO as being representative. When the C and O atoms are not interacting, there are two degenerate $^1\Sigma^+$ states corresponding to the structures

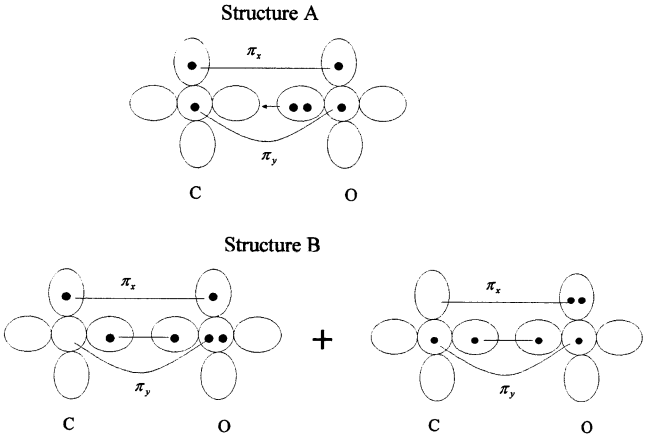

In structure A, the two atoms are both in the $M = 0$ sublevel of the ^3P_g state; in structure B, they are in the $M = \pm 1$ sublevel. Note that these structures define the various spin couplings when the atoms are well separated and are therefore intrinsically multiconfigurational. The asymptotic degeneracy is lifted by the quadrupole−quadrupole interaction, which lowers the energies of both structures (but A preferentially); so at large internuclear separations, the wave function of CO has the character of structure A. This means that the carbon atom has the approximate orbital occupancy $1s^22s^22p_x^12p_y^12p_z^0$ with oxygen being $1s^22s^22p_x^12p_y^12p_z^2$ (z is the internuclear line); so, at this separation, there are 4σ and 2π electrons on carbon and 6σ and 2π electrons on oxygen. The atoms are of course correlated, and although the carbon 2s loses some density to the carbon $2p_z$ via near-degeneracy[32] arguments, the orbital occupations are essentially those corresponding to the restricted open shell Hartree−Fock atomic wave function. Around 3A, the σ bond in structure B begins to develop, the two structures have comparable energies, and because of the overlap of the atomic orbitals, they cease to be noninteracting and begin to mix strongly. Clearly, at equilibrium, the in situ carbon atom has more than 4σ electrons. It has the $1s^2$ pair, the lone pair, and its share of the 2-electron σ bond; so as the CO bond forms, the σ electron population of carbon will increase from its asymptotic value of 4 to something larger. We interpret this as a manifestation of the increasing importance of structure B as the atoms approach their equilibrium separation. Because structure B has 5σ electrons on carbon, we take this to be the limit and anticipate that carbon will have a σ electron population between 4 and 5. Keep in mind that, even though carbon is less electronegative than oxygen, it will gain electrons in the σ system. In a similar way, we imagine carbon going from 2π electrons at large internuclear distances to something less than 2 but greater than 1 at equilibrium. So, although carbon will gain electrons in the σ system, it will lose them in the π system,

and as we will see, it loses more than it gains and has a net positive charge at equilibrium.

The O in structure A has 6σ and 2π electrons, and as the atoms come together and structure B becomes dominant, the number of σ electrons begins to drop (counter to electronegativity expectations), and the π electron population will increase. The increase in the π population is larger than the decrease in that of the σ; therefore, O will have a net negative charge. These observations are also applicable to CS, SiS, and SiO. In each case, S or O loses σ electrons and gains π electrons with the resultant charge being determined by the relative shifts. It is interesting that at large internuclear separations S and O are initially positively charged because the σ loss is initially greater than the π gain. As we will see, this dramatic change in the character of the electronic wave function is evident in all four molecules and is reflected in the rather remarkable intra-atomic charge redistributions between the σ and π orbitals as the bond length deceases.

All electronic structure calculations were done using MOLPRO[33] and an aug-cc-pv5z basis.[34] The orbitals were extracted using the MOLDEN[33] option and subsequently processed using locally written codes.

Atomic Charges. It will be convenient to work with the electron density difference between the molecule, η^{mol}, and the proto-molecule, η^{pm}, rather than with the electron density itself. Accordingly, we define the electron density difference as $\delta\eta = \eta^{\mathrm{mol}} - \eta^{\mathrm{pm}}$ where η^{mol} is the molecular density corresponding to the SCF, CASSCF, or MRCI function and η^{pm} is the proto-molecule density constructed from atomic SCF functions where each of the atomic SCF densities is written as a sum of the σ and π densities.

$$\eta^{\mathrm{pm}} = \eta^0_\sigma(\mathrm{C}) + \eta^0_\pi(\mathrm{C}) + \eta^0_\sigma(\mathrm{O}) + \eta^0_\pi(\mathrm{O})$$

The individual terms are defined as

$$\eta^0_\sigma(\mathrm{C}) = 2\eta^0_{1\mathrm{s}}(\mathrm{C}) + 2\eta^0_{2\mathrm{s}}(\mathrm{C}) + \eta^0_{2\mathrm{p}_z}(\mathrm{C})$$

$$\eta^0_\sigma(\mathrm{O}) = 2\eta^0_{1\mathrm{s}}(\mathrm{O}) + 2\eta^0_{2\mathrm{s}}(\mathrm{O}) + \eta^0_{2\mathrm{p}_z}(\mathrm{O})$$

$$\eta^0_\pi(\mathrm{C}) = 0.5(\eta^0_{2\mathrm{p}_x}(\mathrm{C}) + \eta^0_{2\mathrm{p}_y}(\mathrm{C}))$$

$$\eta^0_\pi(\mathrm{O}) = 1.5(\eta^0_{2\mathrm{p}_x}(\mathrm{O}) + \eta^0_{2\mathrm{p}_y}(\mathrm{O}))$$

Note that we are using oriented atoms rather than the traditional spherically symmetric atoms suggested by Hirshfeld.[19] This means that the electron density of the carbon and oxygen atoms in our proto-molecule is that associated with structure B and corresponds to the electron configurations $1s^2 2s^2 2p_x^{0.5} 2p_y^{0.5} 2p_z^1$ on C and $1s^2 2s^2 2p_x^{1.5} 2p_y^{1.5} 2p_z^1$ on O rather than the spherically averaged configurations $1s^2 2s^2 2p_x^{2/3} 2p_y^{2/3} 2p_z^{2/3}$ on C and $1s^2 2s^2 2p_x^{4/3} 2p_y^{4/3} 2p_z^{4/3}$ on O.

In these oriented atoms, a neutral carbon atom has 5σ and 1π electrons; in contrast, neutral oxygen has 5σ and 3π electrons. When we discuss the charges on a carbon or oxygen atom, it is relative to these references.

The electron density difference, $\delta\eta$, can be partitioned into the σ and π density differences on each atom

$$\delta\eta = \delta\eta_\sigma(\mathrm{C}) + \delta\eta_\pi(\mathrm{C}) + \delta\eta_\sigma(\mathrm{O}) + \delta\eta_\pi(\mathrm{O})$$

where, in the spirit of Hirshfeld,[19] we define

$$\delta\eta_\sigma(\mathrm{C}) = \delta\eta\,\frac{\eta^0_\sigma(\mathrm{C})}{\eta^0_\sigma(\mathrm{C}) + \eta^0_\sigma(\mathrm{O})} = \delta\eta W^\sigma_{\mathrm{c}}$$

$$\delta\eta_\pi(\mathrm{C}) = \delta\eta\,\frac{\eta^0_\pi(\mathrm{C})}{\eta^0_\pi(\mathrm{C}) + \eta^0_\pi(\mathrm{O})} = \delta\eta W^\pi_{\mathrm{c}}$$

$$\delta\eta_\sigma(\mathrm{O}) = \delta\eta\,\frac{\eta^0_\sigma(\mathrm{O})}{\eta^0_\sigma(\mathrm{C}) + \eta^0_\sigma(\mathrm{O})} = \delta\eta W^\sigma_{\mathrm{o}}$$

$$\delta\eta_\pi(\mathrm{O}) = \delta\eta\,\frac{\eta^0_\pi(\mathrm{O})}{\eta^0_\pi(\mathrm{C}) + \eta^0_\pi(\mathrm{O})} = \delta\eta\, W^\pi_{\mathrm{o}}$$

The wave functions have been constructed in C_{2v} symmetry; therefore, the natural orbitals have a_1, b_1, b_2, or a_2 symmetry. We assign those of a_1 symmetry to σ and the those of b_1 and b_2 to π. There are usually fewer than 0.01 electrons in a_2 symmetry, and rather than omit it or carry along an additional symmetry, we have assigned it, arbitrarily, as σ. Additionally, we define the density difference associated with each atom as the sum of the atom's σ and π densities. So, for carbon, we have

$$\delta\eta(\mathrm{C}) = \delta\eta_\sigma(\mathrm{C}) + \delta\eta_\pi(\mathrm{C}) = \delta\eta(W^\sigma_{\mathrm{C}} + W^\pi_{\mathrm{C}})$$

Note that the functions that project the density difference onto the σ and π components of the in situ atoms sum to 1.

$$W^\pi_{\mathrm{c}} + W^\pi_{\mathrm{o}} = W^\sigma_{\mathrm{c}} + W^\sigma_{\mathrm{o}} = 1$$

The charge on carbon and oxygen is written as a sum of σ and π contributions:

$$q(\mathrm{C}) = -\int \delta\eta(\mathrm{C})\,\mathrm{d}V = -\int \delta\eta_\sigma(\mathrm{C})\,\mathrm{d}V - \int \delta\eta_\pi(\mathrm{C})\,\mathrm{d}V = q_\sigma(\mathrm{C}) + q_\pi(\mathrm{C})$$

and

$$q(\mathrm{O}) = -\int \delta\eta(\mathrm{O})\,\mathrm{d}V = -\int \delta\eta_\sigma(\mathrm{O})\,\mathrm{d}V - \int \delta\eta_\pi(\mathrm{O})\,\mathrm{d}V = q_\sigma(\mathrm{O}) + q_\pi(\mathrm{O})$$

The integrals over the various density differences were evaluated numerically. Because the integrands are all cylindrically symmetric, the ϕ integration is analytic, and the θ integration was done using a 48-point Gauss−Legendre quadrature.[35] We used Simpson's rule[35] for the resulting radial integration.

Dipole Moment. The dipole moment can be written as an integral over the density difference[19,20,29]

$$\mu = -\int z\delta\eta\,\mathrm{d}V = -\int z(\delta\eta(\mathrm{C}) + \delta\eta(\mathrm{O}))\,\mathrm{d}V$$

If we have carbon at the origin and oxygen at $z = R$, we may write the atomic dipole on carbon as

$$-\int z\delta\eta(\mathrm{C})\,\mathrm{d}V = \mu(\mathrm{C})$$

with that on oxygen as

$$-\int z\delta\eta(\mathrm{O})\,\mathrm{d}V = \mu(\mathrm{O}) + Rq(\mathrm{O})$$

giving

$$\mu = Rq(\mathrm{O}) + \mu(\mathrm{C}) + \mu(\mathrm{O})$$

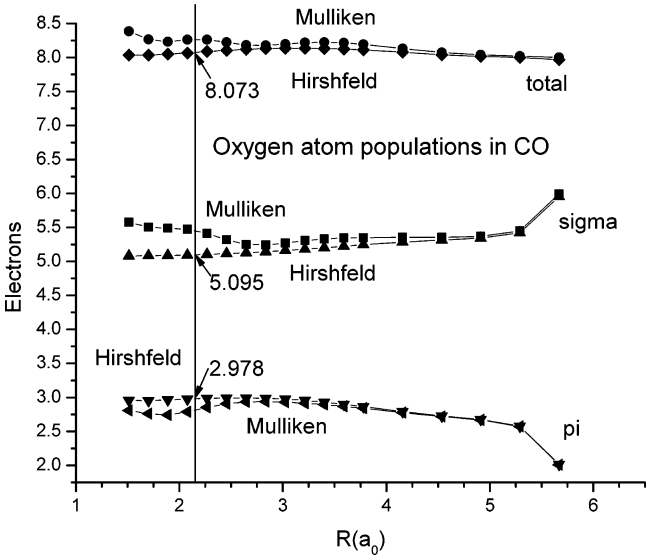

Figure 2. Comparison of the distance dependence of the Mulliken and Hirshfeld electron populations on O in CO calculated with a CASSCF wave function using an aug-cc-pV5Z basis. The vertical line in this and subsequent figures represents the experimental equilibrium internuclear distance.

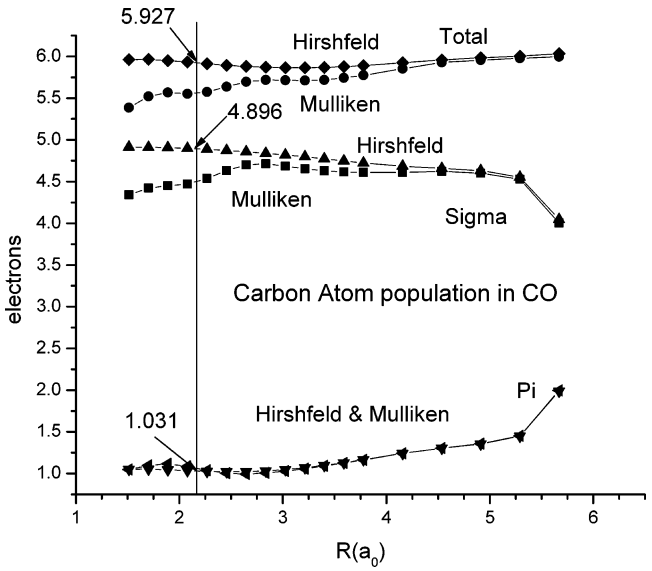

Figure 3. Comparison of the distance dependence of the Mulliken and Hirshfeld electron populations on C in CO. Calculated with a CASSCF wave function using an aug-cc-pV5Z basis.

where the atomic dipoles are evaluated relative to their respective nuclei. Note that like the atomic charges the atomic dipoles can be partitioned into σ and π components.

CO Results. Recall that structure A is the asymptotic ground state, and as the O atom approaches C, it begins with 6σ and 2π electrons. As structure B comes into play, the number of σ electrons begins to drop; in contrast, the number of π electrons on O increases. Because we calculate the charge on an atom relative to structure B, the number of σ and π electrons on O are $N_\sigma(\mathrm{O}) = 5.0 - q_\sigma(\mathrm{O})$ and $N_\pi(\mathrm{O}) = 3.0 - q_\pi(\mathrm{O})$ with the total given by $N(\mathrm{O}) = 8.0 - q_\pi(\mathrm{O}) - q_\sigma(\mathrm{O})$, and these, along with the Mulliken[7] populations, are plotted in Figure 2. As one might expect, the Mulliken and Hirshfeld populations agree at large R where the various interatomic overlaps are small but not at small R where they are significant. Note that both partitionings pick up the large intra-atomic charge shift as structure B begins to mix with structure A. Figure 3 shows this

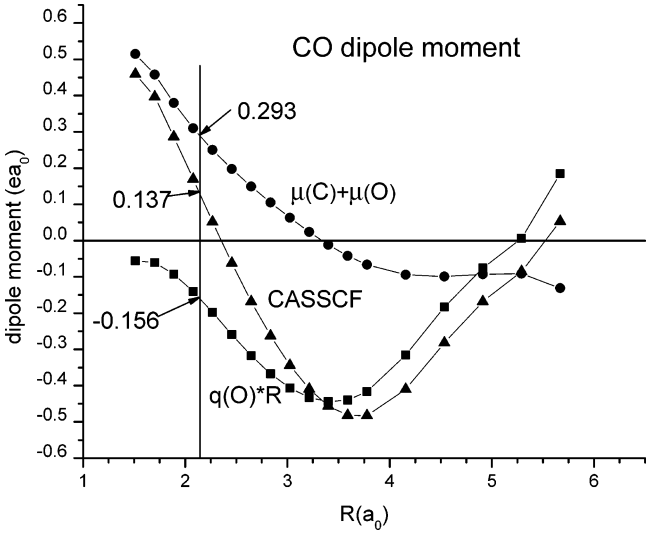

Figure 4. Dipole moment function of CO and its charge and induced dipole components. Calculated with a CASSCF wave function using an aug-cc-pV5Z basis.

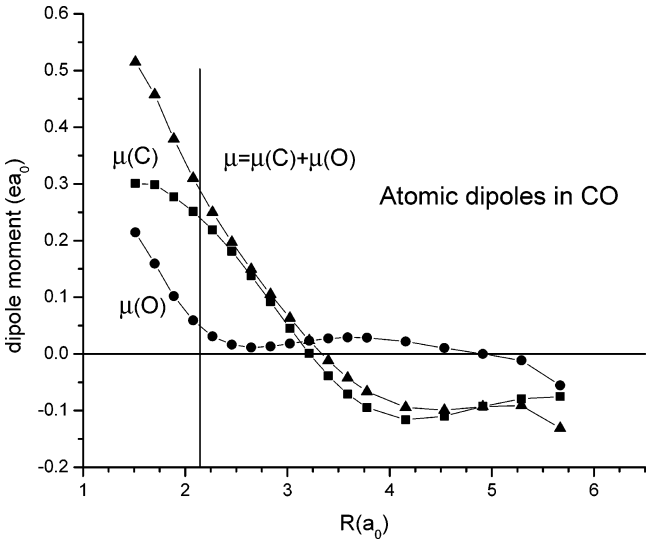

Figure 5. Atomic dipoles in CO. Calculated with a CASSCF wave function using an aug-cc-pV5Z basis.

comparison for carbon. As anticipated, oxygen, at equilibrium, is negative with $q(\mathrm{O}) = -0.0733e$.

The dipole moment function of CO calculated at the CASSCF level is shown in Figure 4 along with its decomposition into the charge, $q(\mathrm{O})R$, and induced atomic dipole, $\mu(\mathrm{C}) + \mu(\mathrm{O})$, contributions. With carbon at the origin, a negative dipole moment corresponds to a C^+O^- polarity. At the experimental bond length, the CASSCF dipole moment is $0.137ea_0$, which we may decompose into $-0.156ea_0$ from the $-0.073e$ charge on O and the $+0.293ea_0$ term from the induced atomic dipoles. It is interesting to see that the minimum in the dipole moment curve results primarily from the $q(\mathrm{O})R$ contribution, which is due to the trade off between σ and π contributions (Figure 2). The induced atomic dipole contribution is decomposed into its carbon and oxygen components in Figure 5 from which we see that the atomic carbon dipole dominates at equilibrium, substantiating our qualitative notion that it is the lone pair on carbon that is responsible for the observed C^-O^+ polarity of the dipole moment. We decompose the carbon atom dipole moment into its σ and π components in Figure 6 where we see that, although the σ component from the lone pair dominates, there is a

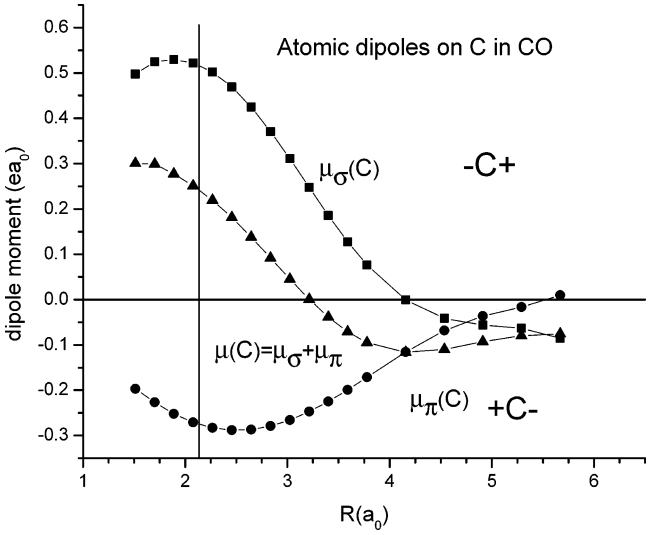

Figure 6. σ and π components of the atomic dipole on C in CO. Calculated with a CASSCF wave function using an aug-cc-pV5Z basis.

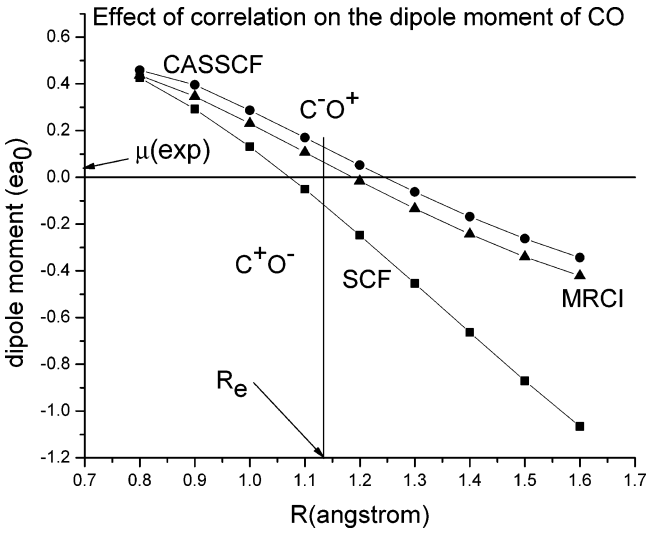

Figure 7. Effect of correlation on the dipole moment of CO. All calculations use an aug-cc-pV5Z basis.

TABLE 2: Comparison of Calculated (aug-cc-pV5Z) and Experimental Dipole Moments (ea_0)

molecule	SCF	CASSCF	MRCI	experiment[a]
C^-O^+	−0.104	+0.137	+0.073	+0.043
C^-S^+	+0.640	+0.814	+0.796	+0.770
Si^+O^-	−1.467	−1.114	−1.178	−1.215
Si^+S^-	−0.894	−0.562	−0.614	−0.681

[a] Experimental dipole moments: CO,[22] CS,[23] SiO,[24] and SiS.[25]

significant dipole due to the shift of π electrons off of the carbon atom and into the bonding region.

Correlation Effects on the CO Dipole Moment. It is well-known[36] that the SCF wave function for CO predicts a dipole moment with polarity C^+O^-, opposite to that observed experimentally, and that correlated wave functions[37,38] are needed to correct this failure. Given our interpretation of the dipole moment, it is of interest to investigate how electron correlation affects the atomic charges and induced atomic moments. Accordingly, we have augmented our CASSCF results with SCF and MRCI (CASSCF+1+2), and the computed dipole moment curves are compared in Figure 7 with the values at equilibrium in Table 2. Although the SCF function predicts a dipole moment of $-0.104ea_0$, the CASSCF ($+0.137ea_0$) and MRCI ($+0.073ea_0$) functions predict a dipole moment that compares favorably to

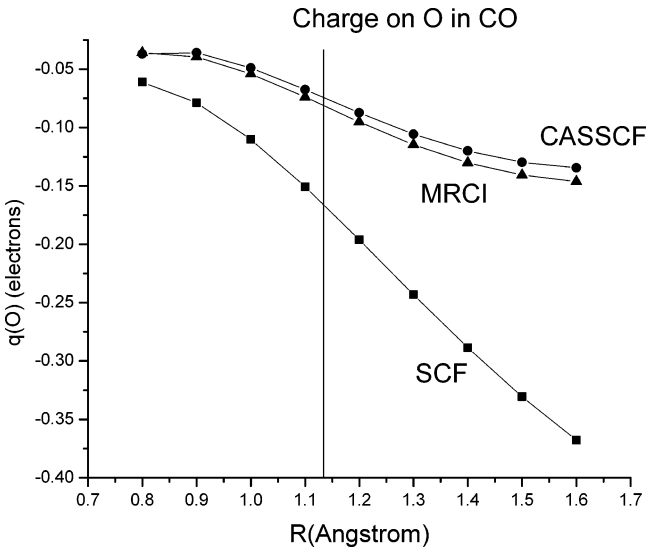

Figure 8. Effect of correlation on the charges on O in CO. All calculations use an aug-cc-pV5Z basis.

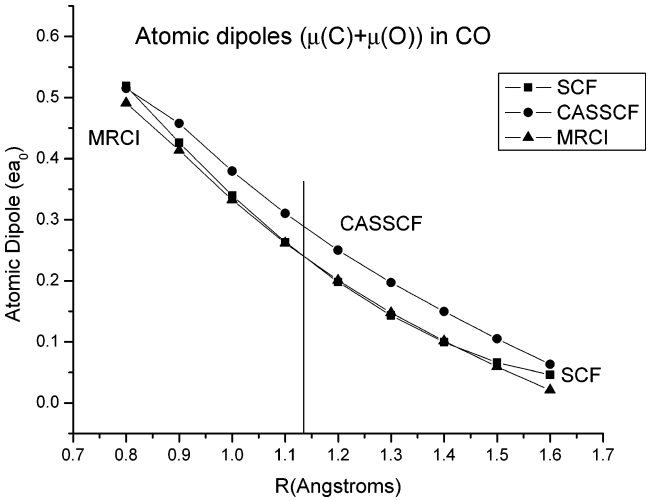

Figure 9. Effect of correlation on the O atomic dipole in CO. All calculations use an aug-cc-pV5Z basis.

TABLE 3: Hirshfeld Charges at Equilibrium from This and Previous Studies

molecule	RHF[a]	CASSCF[a]	MRCI[a]	RHF[b]	DFT[c]
CO	−0.163	−0.073	−0.080	−0.14	−0.080
CS	0.037	0.121	0.119	0.00	0.094
SiO	−0.537	−0.425	−0.421	−0.47	−0.375
SiS	−0.300	−0.212	−0.211		−0.213

[a] This work, aug-cc-pV5Z basis. [b] Reference 20. [c] Reference 17.

the experimental value[22] of $0.04320ea_0$, and clearly, the two correlated wave functions correct the sign problem. In Figure 8, we show the charge on O predicted by the various methods, and it is clear that the SCF function predicts an oxygen charge that is too negative. In contrast, the atomic dipoles shown in Figure 9 are all very similar; therefore, the effect of correlation is to reduce the charge separation in the CO molecule. The charges and the induced atomic dipole contributions of the RHF, CASSCF, and MRCI function are summarized in Tables 3 and 4.

SiS. SiS is the third period counterpart of CO with S being much more electronegative than Si. In Figures 10 and 11, we plot the number of electrons in the σ and π symmetries on Si and S as a function of internuclear separation. As with CO, the more electronegative of the two atoms, S, loses electrons in

TABLE 4: Molecular Dipole Moments Decomposed into the in Situ Charge and Induced Atomic Dipole Contributions

molecule		μ (ea_0)	q(O,S)R (ea_0)	μ(C,Si) (ea_0)	μ(O,S) (ea_0)
C^-O^+	RHF	−0.104	−0.348	+0.218	+0.026
	CASSCF	+0.137	−0.156	+0.243	+0.050
	MRCI	+0.073	−0.171	+0.211	+0.033
	DC[a]	−0.11	−0.308	+0.223	−0.023
C^-S^+	RHF	+0.640	+0.108	+0.202	+0.330
	CASSCF	+0.814	+0.351	+0.207	+0.256
	MRCI	+0.796	+0.344	+0.190	+0.262
	DC[a]	+0.57	+0.010	+0.278	+0.278
Si^+O^-	RHF	−1.467	−1.532	+0.015	+0.050
	CASSCF	−1.114	−1.213	+0.015	+0.084
	MRCI	−1.178	−1.201	−0.043	+0.067
	DC[a]	−1.37	−1.342	+0.044	−0.073
Si^+S^-	RHF	−0.894	−1.094	−0.091	+0.290
	CASSCF	−0.562	−0.773	−0.083	+0.294
	MRCI	−0.614	−0.766	−0.128	+0.282

[a] Davidson and Chakravorty SCF calculations using 6-311G** basis, ref 20.

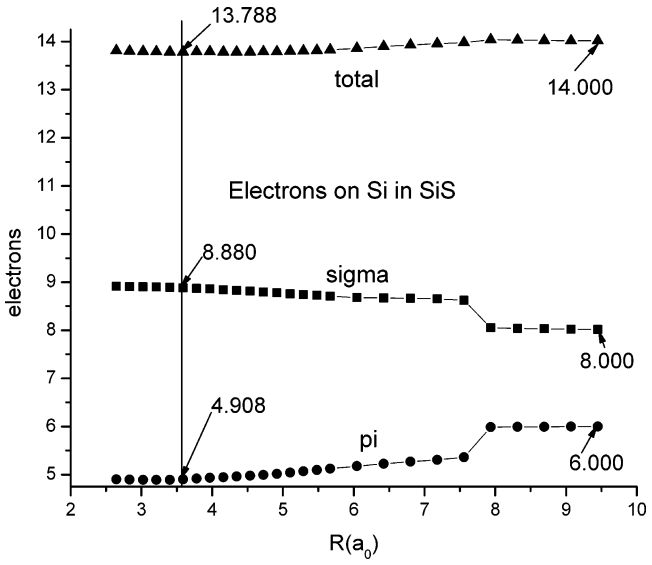

Figure 10. Distance dependence of the Hirshfeld σ and π populations on Si in SiS. Calculated with a CASSCF wave function using an aug-cc-pV5Z basis.

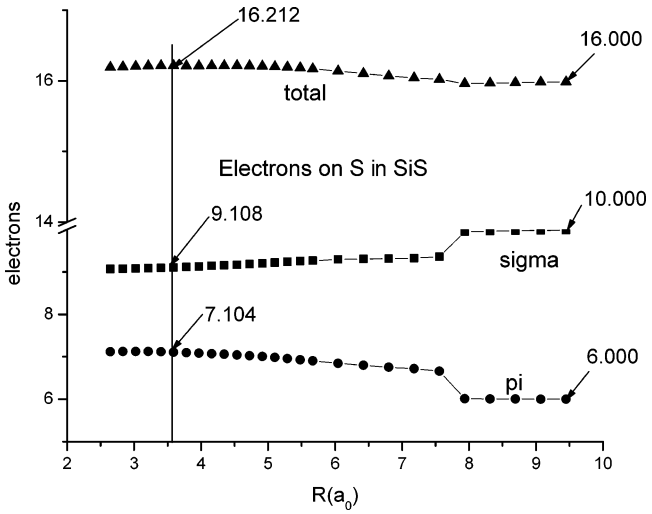

Figure 11. Distance dependence of the Hirshfeld σ and π populations on S in SiS. Calculated with a CASSCF wave function using an aug-cc-pV5Z basis.

the σ system and gains them in the π system as the bond length decreases, consistent with the increased importance of structure B. Additionally, S gains more electrons in π symmetry than it loses in the σ symmetry; therefore, it has a net negative charge.

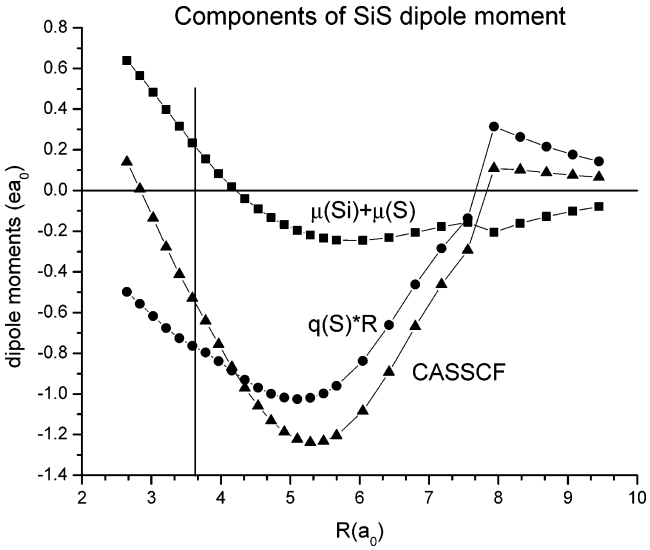

Figure 12. Dipole moment function of SiS and its charge and induced dipole components. Calculated with a CASSCF wave function using an aug-cc-pV5Z basis.

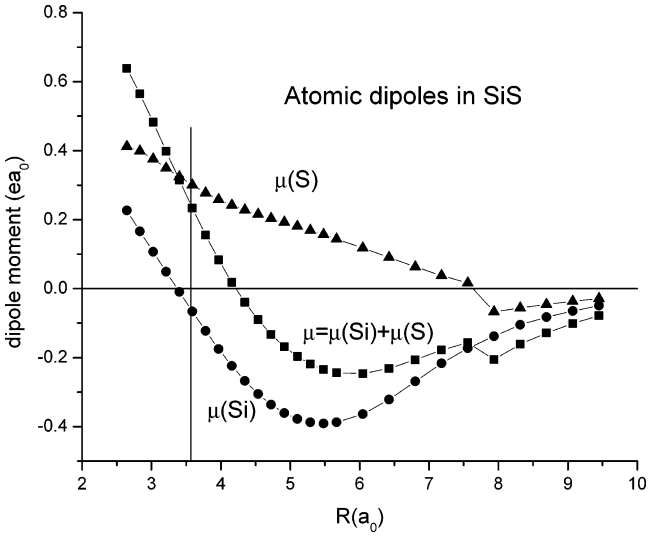

Figure 13. Atomic dipoles in SiS. Calculated with a CASSCF wave function using an aug-cc-pV5Z basis.

The dipole moment function for SiS is shown in Figure 12 along with the charge and induced atomic dipole contributions. As with CO, the minimum in the dipole moment curve comes primarily from the variation of the charge on the more electronegative element (S) with bond length; the minimum is attributable to the opposite flow of electrons in the π and σ systems (Figure 11). The sum of the induced atomic dipoles is opposite in sign to the charge contribution but not large enough to have much of an effect on the dipole moment. Interestingly, when we break the induced atomic dipole into its Si and S components in Figure 13 , we see that Si, like C, is negative and S, like O, is positive, but the relative magnitudes are very different. In CO, C dominated the induced dipole moment, but in SiS, S dominates. The reason for the reduced contribution of Si relative to C can be seen from Figure 14 where we decompose the Si contribution into its σ and π symmetries. Like carbon, silicon has a substantial positive lone pair contribution, but unlike carbon, its negative π contribution almost cancels the lone pair, allowing S to dominate the induced atomic dipole contribution.

Correlation Effects on the Dipole Moment of SiS. The dipole moment curves calculated for SiS with varying degrees

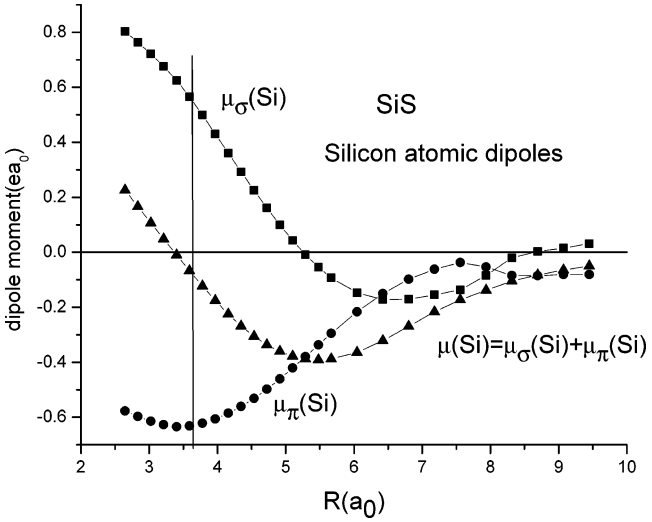

Figure 14. σ and π components of the atomic dipole on Si in SiS. Calculated with a CASSCF wave function using an aug-cc-pV5Z basis.

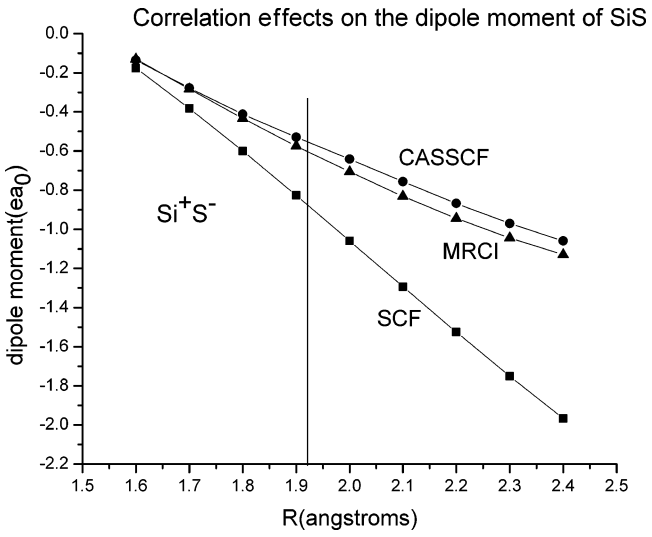

Figure 15. Effect of correlation on the dipole moment of SiS. All calculations use an aug-cc-pV5Z basis.

of correlation are shown in Figure 15 and Table 2. The SCF value of $-0.894ea_0$ is more negative than the experimental value, $-0.681ea_0$; in contrast, the correlated values $-0.562ea_0$ (CASCSF) and $-0.614ea_0$ (MRCI) agree better. From Figure 16 , we see that the primary difference between the SCF and correlated functions is the charge contribution. The SCF charge is $q_{SCF}(S) = -0.300e$, and the MRCI charge is $q_{MRCI}(S) = -0.211e$. As one sees from these numbers, the correlated wave function reduces the charge on S and in particular in the S π system. These results are summarized in Tables 3 and 4.

SiO. The distance dependence of the electron population on the O atom in SiO calculated with the CASSCF wave function is shown in Figure 17. O gains many more electrons in the π system than it loses in the σ system and at equilibrium is quite negative, $q_{MCSCF}(O) = -0.425e$. Figure 18 shows the CASSCF dipole moment function, and we see that at equilibrium the charge component and the atomic dipole moments have opposite signs with the charge component dominating. Figure 19 shows that the small contribution of the induced atomic dipoles is because at equilibrium both atomic dipoles are small.

Correlation Effects in SiO. The dipole moment curves of SiO calculated with various amounts of electron correlation are shown in Figure 20 and Table 1. The SCF value of $-1.467ea_0$

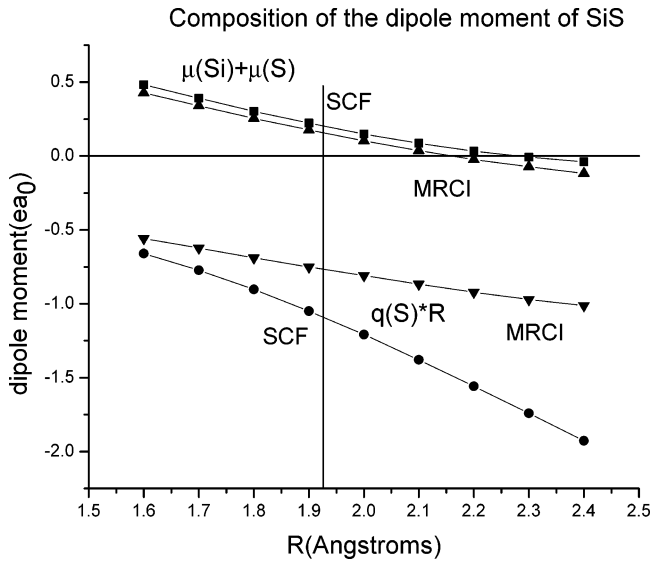

Figure 16. Effect of correlation on the composition of the dipole moment of SiS. All calculations use an aug-cc-pV5Z basis.

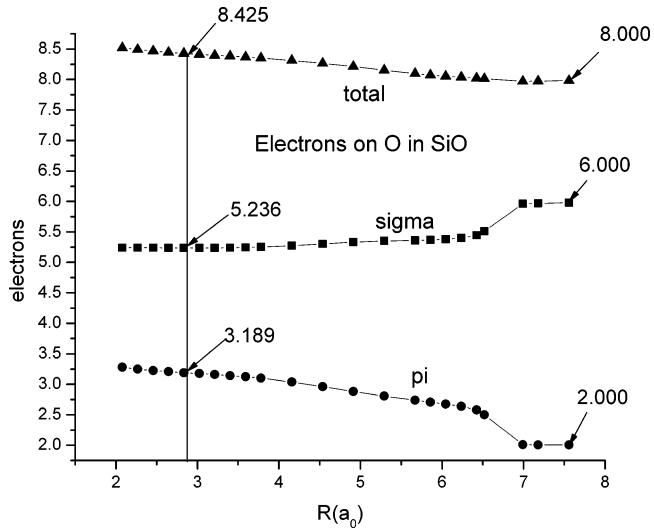

Figure 17. Distance dependence of the Hirshfeld σ and π populations on O in SiO. Calculated with a CASSCF wave function using an aug-cc-pV5Z basis.

is significantly more negative than the experimental value of $-1.215ea_0$; in contrast, the correlated values $-1.114ea_0$ (CASSCF) and $-1.1782ea_0$ (MRCI) agree better. Figure 21 shows that the correlation improves the calculated dipole moment by reducing the charge separation in the molecule. These results are summarized in Tables 3 and 4.

CS. The electron distribution on S in CS is shown as a function of R in Figure 22 where we see the intra-atomic shift of electrons from σ to π as structure A gives way to B. The various charge states of S are emphasized in Figure 23 where the charge on S, $q(S) = N(S) - 16.0$, and C are plotted. The dipole moment curve and its charge and induced moment components are shown in Figure 24. The striking difference between this curve and those of the previous three molecules is the behavior of the charge component. O in SiO and CO and S in SiS are negative, and the charge contribution to their dipole moments reduces the positive induced atomic dipole contribution; in contrast, S in CS is positive and reinforces the induced dipole component, resulting in the substantial dipole moment of C^-S^+ polarity.

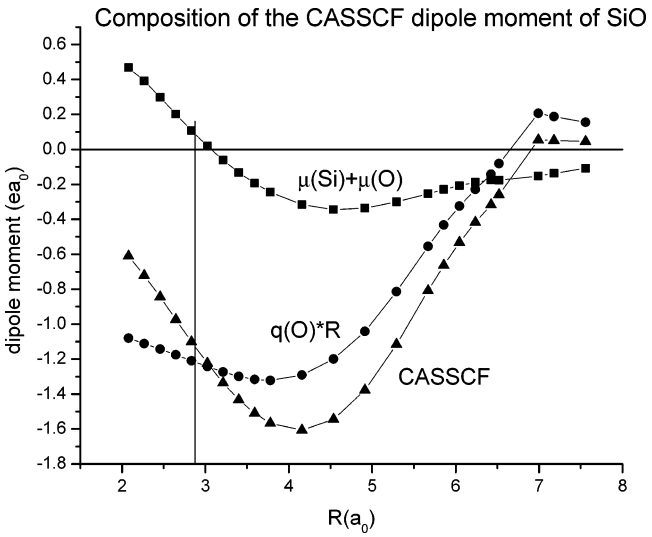

Figure 18. Dipole moment function of SiO and its charge and induced dipole components. Calculated with a CASSCF wave function using an aug-cc-pV5Z basis.

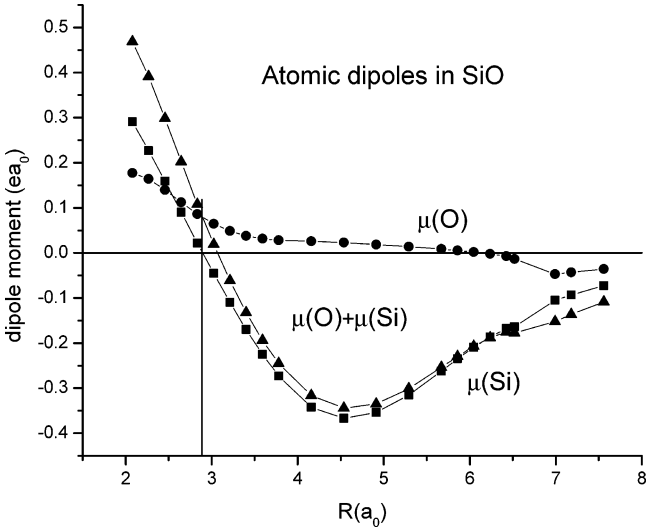

Figure 19. Atomic dipoles in SiO. Calculated with a CASSCF wave function using an aug-cc-pV5Z basis.

Correlation Effects in CS. The dipole moment of CS calculated with various amounts of correlation is shown in Figure 25 and Table 1. Clearly, correlation increases the dipole moment going from $+0.640ea_0$ to $+0.814ea_0$ to $+0.796ea_0$ as we go from the SCF, CASSCF, and MRCI methods, bringing it closer to the experimental value $+0.770ea_0$. We see from Figure 26 that correlation decreases the induced atomic dipoles and increases the charge separation. The equilibrium values of the charges and atomic dipoles for CS are summarized in Tables 3 and 4.

Comparison to Previous Work. There are two previous studies of the Hirshfeld charge distribution in the molecules of interest in this work. The first by Davidson and Chakravorty[20] is an RHF study with a 6-311G** basis in which the proto-molecule was constructed from spherically averaged atoms. These authors report both the atomic charges and the induced atomic dipoles. The second study by Fonseca et al.[17] calculates the Hirshfeld charges using the DFT method with a BP86 functional and a TZ2P basis. The calculated charges from both studies are compared with our results in Table 3. The Davidson−Chakravorty RHF results[20] are consistent with our RHF results, and the DFT charges of Fonseca et al.[17] for CO and SiS are

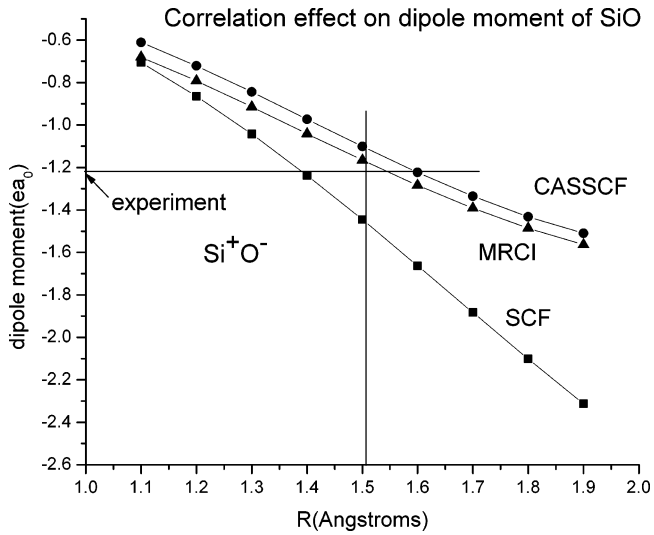

Figure 20. Effect of correlation on the dipole moment of SiO. All calculations use an aug-cc-pV5Z basis.

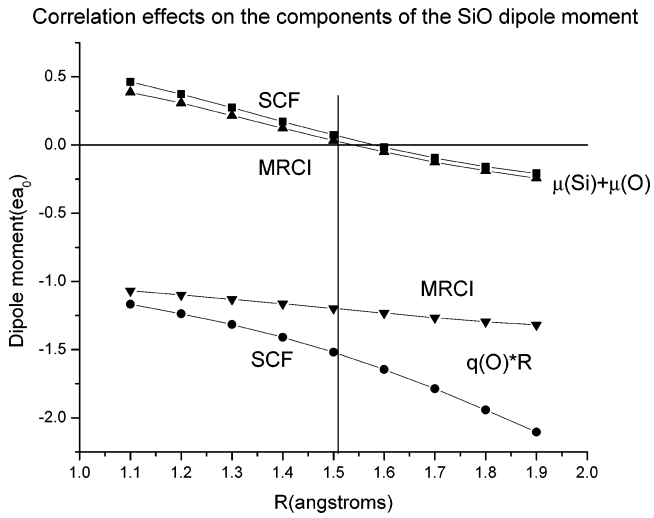

Figure 21. Effect of correlation on the composition of the dipole moment of SiO. All calculations use an aug-cc-pV5Z basis.

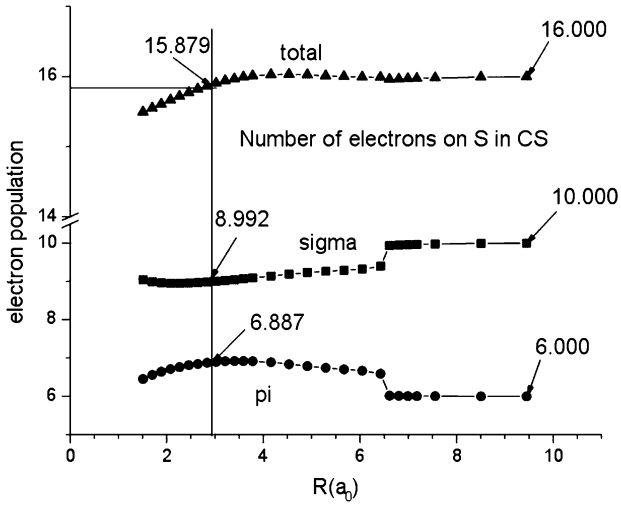

Figure 22. Distance dependence of the Hirshfeld σ and π populations on S in CS. Calculated with a CASSCF wave function using an aug-cc-pV5Z basis.

remarkably similar to our MRCI charges; their charges for the mixed first and second row diatomics SiO and CS are somewhat different but could easily reflect the difference between the

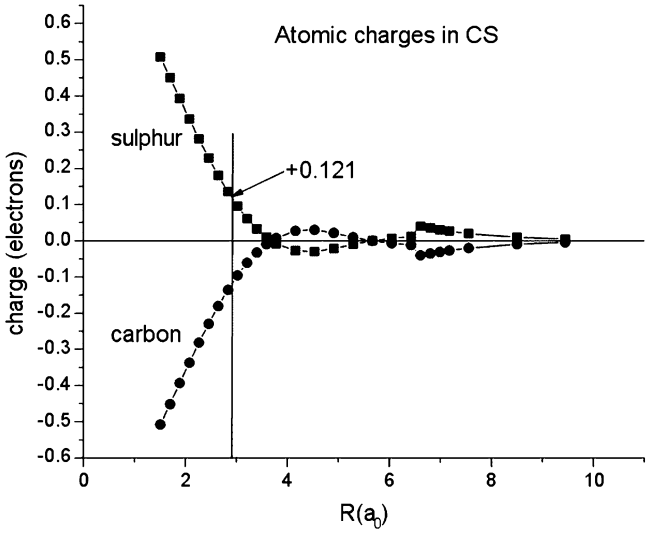

Figure 23. Distance dependence of the atomic charges on C and S in CS. Calculated with a CASSCF wave function using an aug-cc-pV5Z basis.

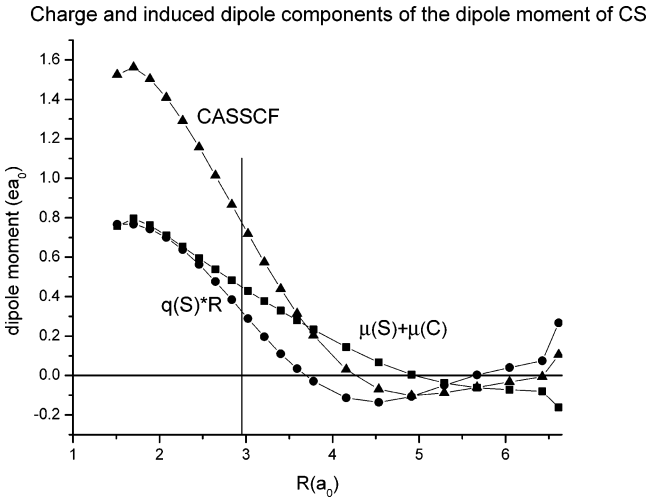

Figure 24. Dipole moment function of CS and its charge and induced dipole components. Calculated with a CASSCF wave function using an aug-cc-pV5Z basis.

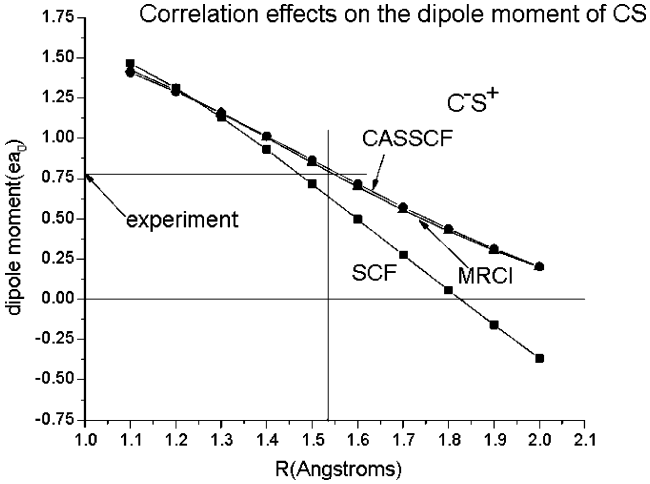

Figure 25. Effect of correlation on the dipole moment of CS. All calculations use an aug-cc-pV5Z basis.

MRCI and DFT densities and our oriented and their spherically averaged proto-molecule. The Davidson and Chakravorty atomic dipoles are compared to our RHF results in Table 4, and the agreement is good, given the difference in the basis set and proto-molecule definition.

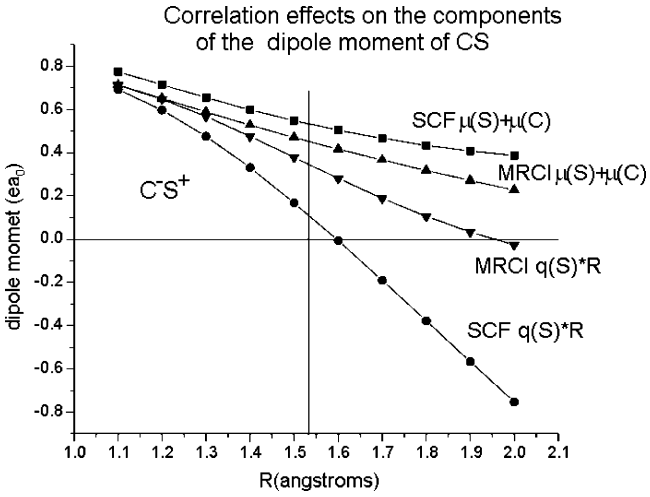

Figure 26. Effect of correlation on the composition of the dipole moment of CS. All calculations use an aug-cc-pV5Z basis.

Summary

The primary findings of this work are:

1. The asymptotic nature of the chemical bond between C or Si and O or S is dictated by the interaction between two $^1\Sigma^+$ states represented symbolically by structures A and B. Their degeneracy at large separations is lifted by the quadrupole−quadrupole interaction, which results in structure A in which both atoms are in the $M = 0$ magnetic sublevels, being the lowest. As the internuclear separation decreases, structure B, corresponding to the $M = \pm 1$ levels, becomes dominant, and there is a transition region where the individual atoms undergo a significant intra-atomic electron shift between the σ to the π system.

2. As the internuclear separation continues to decrease, the σ electron population on O and S decreases; in contrast, the π population increases. The opposite happens with C and Si.

3. The dipole moment of a molecule is determined by the charges and the induced dipoles on the constituent atoms.

4. The dominant effect of electron correlation in these molecules is to make either O or S more positive.

5. In CO, SiO, and SiS, the charge and dipole contributions have opposite polarities; in CS, the two contributions have the same polarity accounting for its anomalously large dipole moment.

6. The dipole moment function of CO, CS, and SiS changes sign because there is an R at which the charge contribution q(O,S)R is negative, and the sum of the induced atomic dipoles is positive, and they cancel.

References and Notes

(1) *Quantum Mechanical Structure Calculations with Chemical Accuracy*; Langhoff, S. R., Ed.; Kluwer Academic Publishers: Dordrecht, Holland, 1995.

(2) Halkier, A.; Larsen, H.; Olsen, J.; Jorgenson, P.; Gauss, J. *J. Chem. Phys.* **1999**, *110*, 734.

(3) Almof, J.; Taylor, P. R. *J. Chem. Phys* **1990**, *92*, 551.

(4) Thakkar, A. J.; Dykstra, C. E. *J. Mol. Struct.: THEOCHEM* **1997**, *400*, 1.

(5) Peterson, K. A.; Dunning, T. H., Jr. *J. Mol. Struct.: THEOCHEM* **1997**, *400*, 93.

(6) Dunning, T. H., Jr; Harrison, R. J.; Feller, D.; Xantheas, S. *Philos. Trans. R. Soc. London, Ser. A* **A2002**, *360*, 1079.

(7) (a) Mulliken, R. S. *J. Chem. Phys*. **1955**, *23*, 1833. (b) Mulliken, R. S. *J. Chem. Phys.* **1955**, *23*, 1841. (c) Mulliken, R. S. *J. Chem. Phys*. **1955**, *23*, 2338. (d) Mulliken, R. S. *J. Chem. Phys.* **1955**, *23*, 2343.

(8) Stone, A. J. *The Theory of Intermolecular Forces;* Clarendon Press: Oxford, U.K., 1996.

(9) Stone, A. J.; Alderton, M. *Mol.. Phys*. **1985**, *56*, 1047.

(10) Mulliken, R. S. *J. Chem. Phys*. **1961**, *36*, 3428.

(11) Noell, J. O. *Inorg. Chem*. **1982**, *21*, 11.

(12) Bauschlicher, C. W., Jr.; Bagus, P. S. *J. Chem. Phys*. **1984**, *81*, 5889.

(13) Chang, H; Harrison, J. F.; Kaplan, T. A.; Mahanti, S. D. *Phys. Rev. B* **1994**, *49*, 15753.

(14) Harrison, J. F. *Mol. Phys.* **2005**, *103*, 1099.

(15) Stone, A. J. *J. Chem. Theory. Comput.* **2005**, *1*, 1128.

(16) Voronoi, G. F.; *J. Reine Angew. Math.* **1908**, *134*, 198.

(17) Guerra, C. F.; Handgraaf, J.; Baerends, E. J.; Bickelhaupt, F. M. *J. Comput. Chem*. **2003**, *25***,** 189.

(18) Bader, R. F. W. *Atoms in Molecules. A Quantum Theory*; Clarendon Press: Oxford, U.K., 1990.

(19) Hirshfeld, F. L. *Theor. Chim. Acta* **1977**, *44*, 129.

(20) Davidson, E. R.; Chakravorty, S. *Theor. Chim. Acta* **1992**, *83*, 319.

(21) Harrison, J. F. *J. Phys. Chem. A* **2005**, *109*, 5492.

(22) Muenter, J. S. *J. Mol. Spectrosc.* **1975**, *55*, 490.

(23) Winnewisser, G.; Cook, R. L. *J. Mol. Spectrosc*. **1968**, *28*, 266.

(24) Raymonda, J. W.; Muenter, J. S.; Klemperer, W. A. *J. Chem. Phys*. **1970**, *52*, 3458.

(25) Hoeft, J.; Lovas, F. J.; Tiemann, E.; Torring, T. *Z. Naturforsch., A: Phys. Sci*. **1969**, *22*, 1422.

(26) Hueber, K. P.; Herzberg, G. *Molecular Spectra and Molecular Structure, Constants of Diatomic Molecules*; Van Nostrand: Princeton, NJ, 1979.

(27) Allen, L. C. *J. Am. Chem. Soc*. **1989**, *111*, 9003.

(28) Huzinaga, S.; Miyoshi, E.; Sekiya, M. *J. Comput. Chem*. **1993**, *14*, 1440.

(29) Harrison, J. F. *J. Chem. Phys*. **2003**, *119*, 8763.

(30) Langhoff, S. R.; Bauschlicher, C. W., Jr. *J. Chem. Phys*. **1995**, *102*, 5220.

(31) Maroulis, G.; Makris, C.; Xenides, D.; Karamanis, P. *Mol. Phys.* **2000**, *98*, 481.

(32) Clementi, E.; Veillard, A. *J. Chem. Phys*. **1966**, *44*, 3050.

(33) Werner, H. J.; Knowles, P. J.; Almof, J.; Amos, R. D.; Deegan, M. J. O.; Elbert, S. T.; Hampel, C.; Meyer, W.; Peterson, K.; Pitzer, R.; Stone, A. J.; Taylor, P. R.; Lindh, R.; Mura, M. E.; Thorsteinsson, T. *Molpro*, a package of ab initio programs.

(34) Dunning, T. H. Jr., *J. Chem. Phys*. **1989**, *90*, 1007.

(35) Abramowitz, M.; Stegun, I. A. *Handbook of Mathematical Functions*; Dover Publications, Inc.: New York, 1970.

(36) Huo, W. H. *J. Chem. Phys*. **1965**, *43*, 624.

(37) Green, S. *J. Chem. Phys*. **1971**, *54*, 624.

(38) Grimaldi, F.; Lecourt, A.; Moser, C. *Intern. J. Quantum. Chem*. **1967**, *1S*, 153.